Vibration based baseline updating method to localize crack formation and propagation in reinforced concrete members

Abstract

Structural Health Monitoring (SHM) schemes are useful for proper management of the performance of structures and preventing their catastrophic failures. Future SHM schemes will inevitably include a robust and automated damage assessment technique to detect, localize and quantify damage. In this context, SHM research has focussed on vibration based damage assessment techniques (VBDATs). Although, damage assessment using VBDATs have been able to achieve reasonable success for structures made of homogeneous materials such as steel, the same success level has not been reported with respect to Reinforced Concrete (RC) structures. The complexity of flexural cracks is claimed to be the main reason to hinder the applicability of existing VBDATs towards RC structures. To address this situation, this paper presents a novel method that has been developed as part of a comprehensive research project carried out at Queensland University of Technology, Brisbane, Australia. Results indicate that use of a constant baseline throughout the damage assessment process undermines the potential of Modal Strain Energy based Damage Index (MSEDI). A novel process, which is referred as the baseline updating method, is therefore devised. This proposed method continuously updates the baseline and systematically tracks both crack formation and propagation. The versatility of this baseline updating method is successfully verified against different crack formation and propagation patterns.

Key words

Baseline updating method, damage index, reinforced concrete structures, flexural cracks, crack formation, crack propagation, damage localization.

1. Introduction

Establishing safer performance levels of structures has been a dominant subject matter for many decades to minimise the negative effects on social and economic development of a society while saving human lives. In this context, Structural Health Monitoring (SHM) has emerged as a means of monitoring the performance of a structure and detecting the onset of damage so that appropriate retrofitting may be carried out to prevent the collapse of the structure. Research in vibration based damage assessment techniques (VBDATs) has been a major part of SHM research during the past two decades. Technological developments such as wireless sensors, high speed computers and modern data acquisition systems have expedited the research on vibration based damage assessment techniques (VBDAT). Non-destructive nature and minimum hindrance to the functionality of the structure are the main attributes that promote VBDATs over other damage assessment methods.

VBDATs use changes in vibration properties between two states to identify existence, location and severity of damage with or without using a computer model [1-3]. In this context, Damage Index (DI) methods based on the modal properties of a structure, are straightforward, fast, inexpensive and have the ability to automate the damage assessment process [4]. Further, they can successfully assess damage using real measurements alone and hence classified as a non-model, response or output based VBDAT [2, 4, 5]. Although DI methods have been mostly successful in detecting and localizing single and multiple damage in structures made of homogeneous materials such as steel [6, 7], their potential to assess damage in RC structures has been limited [8].

The complex damage pattern of RC structures is the main cause that reduces the damage assessment ability of DI methods. Some other reasons are sensitivity to environmental variations, creep and shrinkage effects, modelling difficulties arising from non-homogeneity

and lack of experimental investigations, all which are beyond the scope of the present paper. The predominant damage type, flexural cracks, in RC structures propagates non-uniformly in orthogonal directions. More specifically, flexural cracks have a propensity to spread in longitudinal and/or transverse directions than in the depth direction, due to the presence and effect of tensile reinforcement. Therefore, widely spread crack zones are more prominent in RC structures under flexural loading. Severity of such cracks reduces non-uniformly with distance from the centre or the crack initiation point. Change in load pattern and magnitude may cause the formation of new cracks and/or propagation of existing cracks. This complex behaviour in cracked RC structures has not been adequately investigated in the research context of VBDATs [8].

The present study addresses this knowledge gap and proposes a technique to improve the overall damage assessment ability. The developed method has the ability to automate the damage assessment process with enhanced accuracy in assessing damage in RC structures using the DI Method.

1.1. Damage Index Method

DI method evaluates changes in vibration properties of the structure between two states using a comparative indicator, which is named as the Damage Index (DI). A large number of DIs have been proposed in the literature based on different types of vibration properties such as frequencies [7, 9-11], damping factors [12, 13], mode shapes [4, 14-17], derivatives of mode shapes [5, 18, 19], flexibility values [20, 21], flexibility curvatures [22] and modal strain energy values [23-26]. The first state where the vibration properties are measured defines the baseline, whereas all subsequent measurements correspond with evaluation states of the damage assessment process. Vibration properties of the undamaged structure are most

commonly used to define the baseline. Alternatively, vibration properties at the best known healthy state or computer simulations are used, if the undamaged state is not attainable, such as in case of existing structures. Existing DI methods do adhere to a single baseline during the damage assessment process and hence the authors classify them as constant baseline methods in this paper.

Firstly, this paper evaluates damage localization ability of the constant baseline method using the Modal Strain Energy based Damage Index (MSEDI). Findings of this study highlights that MSEDI does not detect and locate sequentially propagating flexural cracks in RC structures, with respect to a constant baseline. A baseline updating method was therefore developed as a part of a comprehensive SHM research project carried out at Queensland University of Technology (QUT), Brisbane, Australia [8]. Improved damage localization ability of this method was then verified using different crack patterns such as overlapped cracks, formation of new cracks and propagation of existing cracks. Section 2 of this paper presents details of the proposed baseline updating method. Details of the crack patterns and verification of improved damage localization ability of the proposed baseline updating method are presented in section 3.

2. Proposed baseline updating method

2.1. Damage Index

The baseline updating method presented in this paper uses the Modal Strain Energy based Damage Index (MSEDI) proposed by Wahalathantri et al. [26] due to its superior damage localization abilities. However, all steps presented in this paper can easily be replaced with a different damage index, if there is a need.

Equation 1 represents the MSEDI is based on individual modes. It should be noted that generalized subscripts 'b' and 'e' have been used to denote baseline and evaluation states, instead of commonly used subscripts 'h' and 'd' for healthy and damaged states as used with existing or constant baseline methods.

$$\beta_{ji}=\left\{\frac{\left(\int_{X_j}^{X_{j+1}}\{\varphi_i''\}^2\,dx\right)_e+\left(\int_0^L\{\varphi_i''\}^2\,dx\right)_e}{\left(\int_{X_j}^{X_{j+1}}\{\varphi_i''\}^2\,dx\right)_b+\left(\int_0^L\{\varphi_i''\}^2\,dx\right)_b}\times\frac{\left(\int_0^L\{\varphi_i''\}^2\,dx\right)_b}{\left(\int_0^L\{\varphi_i''\}^2\,dx\right)_e}-1\right\}\times\left[\frac{\left|(\varphi_{ji}'')_b\right|}{\left|(\varphi_{ji}'')_b\right|_{max}}\right] \quad \textbf{Equation 1}$$

In the above equation, β_{ji} is the MSEDI at element "j" for mode "i", j = element number, i = i^{th} mode, X_j & X_{j+1} = X co-ordinates of j^{th} and $j+1^{th}$ element, ϕ_i'' = second derivative of i^{th} mode shape, L = total length of the beam, e = evaluation state, b = baseline state, | | and 'max' stand for the absolute and maximum values.

Equation 2 shows the MSEDI at location "j" for a combination of multiple modes [26]. MSV_i is the modal sensitivity value proposed by Lee et al. [27] to assign different weights based on the sensitivity of the mode to the damage. Equation 3 defines MSV_i, in which λ_i is the Eigen-value of the mode 'i'.

$$\beta_j=\sum_1^i\{\beta_{ji}x\ MSV_i\} \quad \text{Equation 2}$$

$$MSV_i = \frac{\frac{\left\{\sum\left[(\varphi_{ji})_e\right]^2\right\}^{0.5}}{(\lambda_i)_e}-\frac{\left\{\sum\left[(\varphi_{ji})_b\right]^2\right\}^{0.5}}{(\lambda_i)_b}}{\frac{\left\{\sum\left[(\varphi_{ji})_b\right]^2\right\}^{0.5}}{(\lambda_i)_b}} \quad \text{Equation 3}$$

2.2. Baseline Updating Method

The proposed baseline updating method conforms with the common definition of damage as a degradation of structural performance between two states. This definition does not imply that the damage should always be measured with respect to a constant baseline. In other

terms, the baseline can be updated to a different state of the structure during the evaluation states. This sets the hypothesis of the proposed baseline updating method presented in this paper. The proposed baseline updating method has two phases: phase 1 and phase 2. The steps involved in phases 1 and 2 are illustrated in Figures 1 and 2 respectively.

Some important terminologies of the proposed baseline updating method are explained below

Primary baseline (BL_P): Initial vibration properties (i.e. mode shapes and frequencies for the MSEDI) of the structure at a known state.

Evaluation state (ES): Vibration properties obtained at state/s where the structural health needs to be assessed.

Damaged state (DS): The current evaluation state is called as the damaged state, if damage is detected.

Secondary baseline (BL_S): A new baseline should be defined as soon as a new damage state is detected (when the evaluation state becomes a damage state). This new baseline is referred to as the secondary baseline.

2.2.1. Phase 1: Detecting the first damage

The baseline updating method starts with defining the primary baseline, BL_P, which is the first step of phase 1 as shown in Figure 1. Vibration properties, namely, mode shapes and frequencies, of the undamaged structure should be recorded for BL_P under all possible situations. In all other cases, vibration properties from computer simulations or the best known state can be used as alternative sources for BL_P. The second step is obtaining the same vibration properties at evaluation states, ES_k, where the subscript k = 1, 2, 3,.... is used to denote the number of evaluations.

Third step in phase 1 is the condition evaluation. A positive β_j value indicates that the j^{th} element is subjected to damage at the current evaluation state, ES_k, with respect to the

primary baseline, BL_P, in the absence of measurement noise. The Generalized Damage Localization Index (GDLI) proposed by Wahalathantri et al. [26] can be used to confirm the damaged state for cases with noisy measurements. This paper uses numerical simulation results to validate the proposed baseline updating method and hence does not treat cases with measurement noise. The number of damaged elements and the magnitude of β_j depend on the extent and the severity of the damage, respectively. Absence of positive β_j indicates that the structure is intact with respect to BL_P.

First three steps are repeated in the existing constant baseline methods throughout the damage evaluation process, whereas the proposed baseline updating method repeats these three steps only until the first damage is detected. Once the first damage is detected, a secondary baseline, BL_S, is introduced to the damage assessment process as shown in step 4. In addition, a matrix denoted by $[DE]_{Nx1}$ is defined to save the diagnosed damaged elements and their damage index values. Number of rows, N, of the matrix [DE] is the total number of elements. Entry for the j^{th} row in first column of this matrix (i.e. $DE_{j,1}$) is defined in Equation 4. The damage assessment process should then be continued with the phase 2.

$$DE_{j,1} = \begin{cases} \beta_j; & \beta_j > 0 \\ 0,; & \beta_j \leq 0 \end{cases} \qquad \text{Equation 4}$$

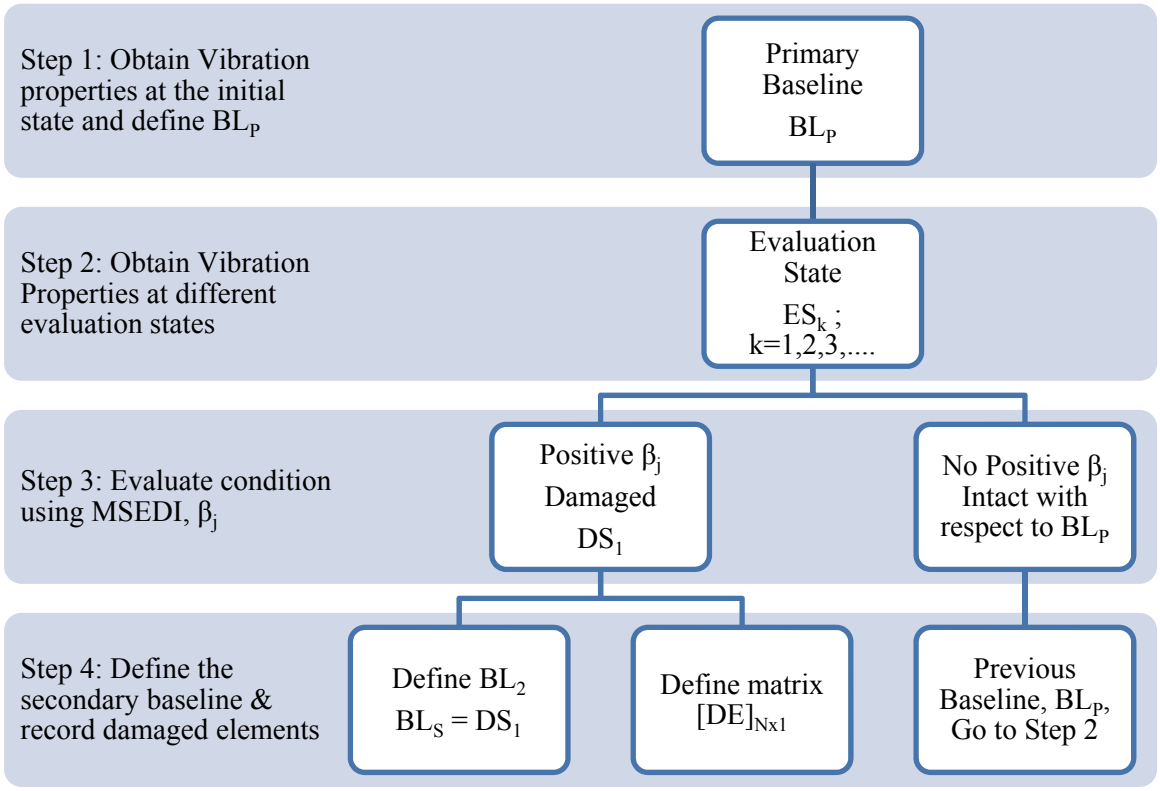

Figure 1: First phase of the proposed baseline update method

2.2.2. Phase 2

Figure 2 illustrates steps of the second phase that starts with two baselines, namely, BL_P and BL_S, and two matrices, $[DE^P]$ and $[DE^S]$. These two matrices initially set to the first column entries of matrix [DE] of step 4 in phase 1 and should be updated if a new damage state is detected during step 7 to track the history of damage formation and propagation.

In step 5, the DI values, β_j, are calculated (at each of the evaluation stages, ES_k) with respect to both primary and secondary baselines. Next, the structure is evaluated to diagnose for crack formation and/or propagation. Presence of positive β_j values with respect to the secondary baseline, BL_S, is an indication of crack formation and/or propagation. Otherwise, structure has not been subjected to further damage, i.e. crack propagation and/or formation,

with respect to the last known damaged state and hence steps 5 onwards should be repeated without updating the secondary baseline, BL_S and matrices, $[DE^P]$, $[DE^S]$ and $[DE]$.

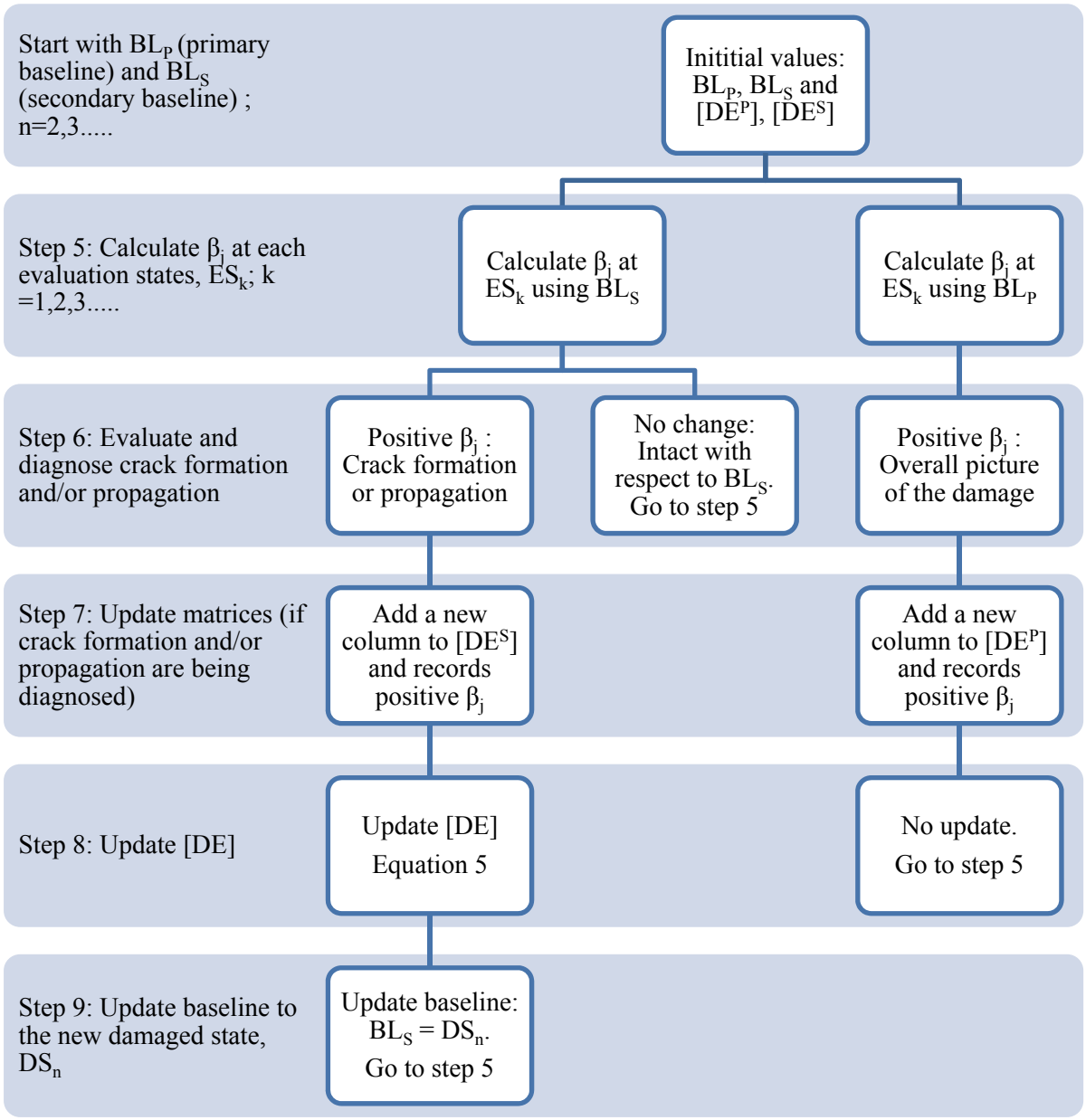

Figure 2: Second phase of the proposed baseline update method

Step 7, 8 and 9 are performed once the structure is diagnosed with crack formation and/or propagation. First, a new column is added to each of two matrices, $[DE^P]$ and $[DE^S]$, as shown in step 7. The new matrices (with the added column) can therefore be represented by $[DE^P]_{N \times n+1}$ and $[DE^S]_{N \times n+1}$, in which n ($\geq$1) represents the total number of baseline updating

carried out in the damage assessment process. The j^{th} row entry of the newly added column is assigned with β_j if β_j is positive or else with zero. β_j of $[DE^S]$ and $[DE^P]$ should be calculated with respect to secondary and primary baselines respectively.

In the next step, the matrix [DE] is updated using Equation 5 to record all damaged elements up to the current evaluation state. A cumulative damage index $\beta_{c,j}$ as given in Equation 6 is then calculated to locate all damage elements with enhanced visual diagnosis. Finally, in step 9, the secondary baseline is updated to the new damaged state, DS_n. Step 5 onwards should then be repeated throughout the damage assessment process.

$$DE_{j,1} = \begin{cases} DE_{j,1} + \beta_j \; ; \; \beta_j > 0 \\ DE_{j,1} \quad ; \; \beta_j \leq 0 \end{cases} \qquad \text{Equation 5}$$

In the above equation, the damage index values, β_j, are calculated with respect to the secondary baseline, BL_S.

$$\beta_{c,j} = \begin{cases} \dfrac{1}{\log\left(1/DE_{j,1}\right)} \; ; \; DE_{j,1} > 0 \\ 0 \qquad\quad ; \quad DE_{j,1} \leq 0 \end{cases} \qquad \text{Equation 6}$$

3. Case studies

This section evaluates the damage localization abilities of the constant baseline method and the proposed baseline updating method using five case studies. The first four case studies represent formation of cracks in a sequential order at two locations with different damage severities. The last case study represents a typical case where crack formation and propagation occur at three locations.

Section 3.1 presents the finite element modelling attributes, whereas section 3.2 presents details of the five case studies, crack patterns and damage localization results of the constant baseline method and the proposed baseline updating method.

3.1 Damage simulation

A RC beam model is used throughout this study. Details of this RC beam model are given in section 3.1.1. Section 3.1.2 briefly presents the damage simulation technique used for all case studies.

3.1.1. Details of the RC beam model

A finite element model of a simply supported RC beam is used for all case studies. Length, width and depth of the RC beam are 4.54m, 0.22m and 0.32m, respectively. Reinforcement arrangement is illustrated in Figure 3. T6 and T12 are 6mm and 12mm diameter reinforcement bars with yield strength, elastic modulus and density of 510MPa, 210GPa and 7850kg/m^3 respectively. Compressive strength, elastic modulus (flexural) and density of concrete are taken as 32MPa, 38.9GPa and 3200kg/m^3 respectively.

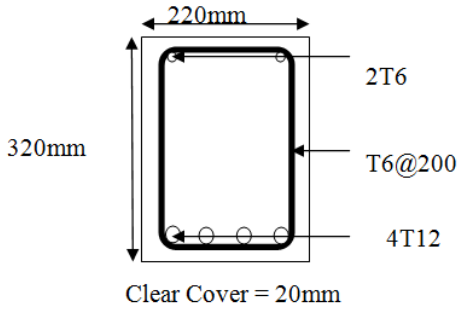

Figure 3: Cross section details of the RC beam model

3.1.2. Damage simulation

Flexural cracking in RC members was simulated using ABAQUS damaged plasticity material model [28]. Accuracy of the ABAQUS damaged plasticity model has been previously established by the authors [29]. Two stress-strain curves for concrete under compression and tension, including damage parameters are required to define the damaged plasticity model.

These two curves have been previously developed and validated by the authors [8, 26] for the RC beam setup used in this paper.

All crack zones simulated in this study were created by applying concentrated point loads. Different loading and unloading patterns were used to simulate sequential crack formation and/or propagation. Figure 3 shows the typical loading arrangement for simulating load induced flexural cracks for the first four case studies. The concentrated load W_1 was initially applied to induce the first flexural crack at a distance of X_{W1} from the left end. Next, W_1 was fully unloaded as shown in step 2. This was followed by the second loading step to apply W_2 and induce the second crack at a distance of X_{W2}. Finally, the W_2 was unloaded. Four finite element models were developed for the different W_1, X_{W1}, W_2 and X_{W2} to simulate the first four case studies. Alternative loading and unloading sequences were used during the fifth case study including a third loading point to form a new cracking zone at a distance of X_{W3} under a point load of W_3.

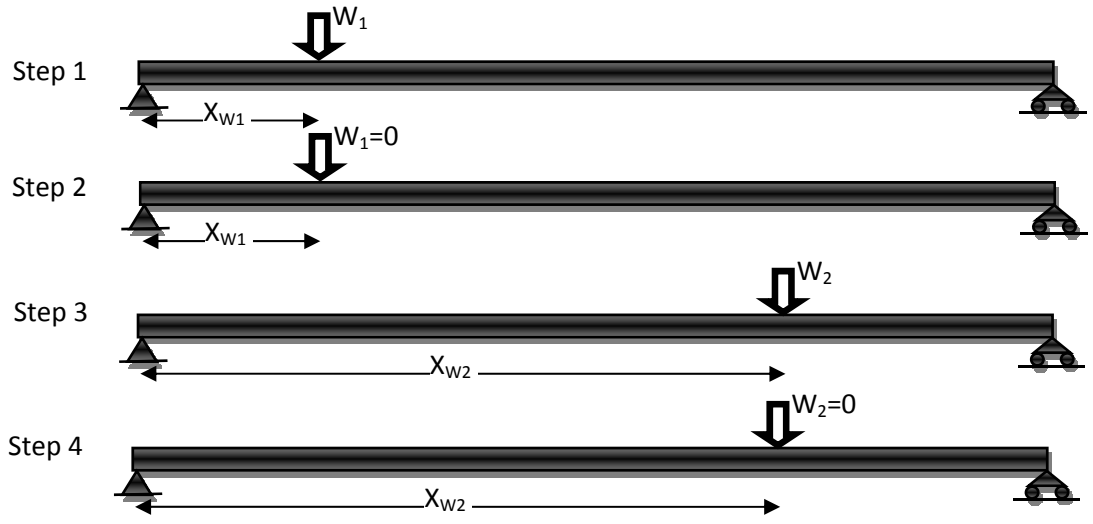

Figure 3: Loading arrangements for case studies 1-4.

3.1.3. Damage index calculation

Using free vibration analysis of the finite element models mentioned above, frequencies and mode shapes of first four modes are first obtained at the undamaged state to define the primary baseline, BL_P, and then the same vibration properties at each of the damaged states are obtained to define evaluation states, ES_k. It should be noted that, modal displacement values at equally spaced 31 nodes are used to calculate MSEDI, β_j, of 30 elements. These 30 elements are numbered from 1 to 30 from left to right. The present study does not consider any intermediate crack propagation stages during a loading step as well as the noise effect. The damaged states, DS_k, are therefore identical to the evaluation states, ES_k. This means the first evaluation state, ES_1, and first damaged state, DS_1, correspond to the damaged structure after the first loading step. Similarly, ES_2 and DS_2 correspond with the damaged structure after the second loading step for all five case studies. Additional evaluation and damaged states are defined for the fifth case study at end of the each loading step.

In all case studies, damaged elements or the tensile crack zones are first identified using the tensile damage parameter, DAMAGET, from the ABAQUS [28] simulation, so that the damage localization ability of the constant baseline and proposed baseline update methods are correctly assessed.

3.2. Case study 1: Higher damage at mid span followed by lower damage at quarter span

A point load, W_1=60kN, is first applied at the mid span (i.e. X_{W1}=2.270m) to form the first crack that extends over elements 9 – 23 as shown in Figure 4. W_1 is then unloaded before applying the second point load, W_2 of 42kN, at quarter span (i.e. X_{W2}=1.135m). The first case study hence represents the onset of a crack around the quarter span of the RC beam that has

been previously subjected to a crack at mid span. Load values are cautiously selected in such a manner that the severity of the first crack is greater than that of the second crack. Figure 5 shows the ABAQUS DAMAGET parameter and identified damaged elements after the second loading step. It should be noted that the second crack forms within the first crack zone and hence any differences between figures 4 and 5 are hardly visible. But, comparison of DAMAGET values clearly depicts that a new crack has formed at quarter span.

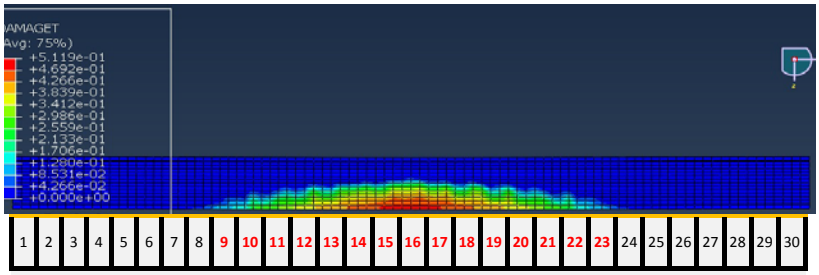

Figure 4: ES_1 of case study 1 - Cracked zone after first loading step

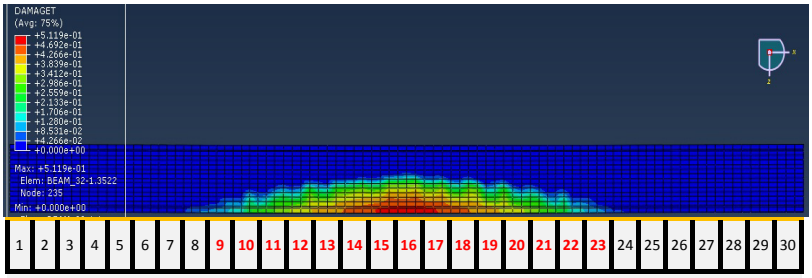

Figure 5: ES_2 of case study 1 - Cracked zone after second loading step

3.2.1. Damage localization results using constant baseline method

The constant baseline method assesses damage with respect to the primary baseline, BL_P, throughout. The damage index values, β_j, of 30 elements at the two evaluation states, ES_1 and ES_2, are therefore calculated with respect to BL_P and plotted in Figure 6 and 7, respectively.

Positive β_j values in Figure 6 around elements 11-20 proves that β_j has accurately localized the first damage zone at ES_1. Figure 7, which plots the β_j values after the second loading step is more or less similar to Figure 6 and hence does not indicate any positive values around the

quarter span. This proves that the constant baseline method fails to localize the onset of a crack if the structure has been previously damaged.

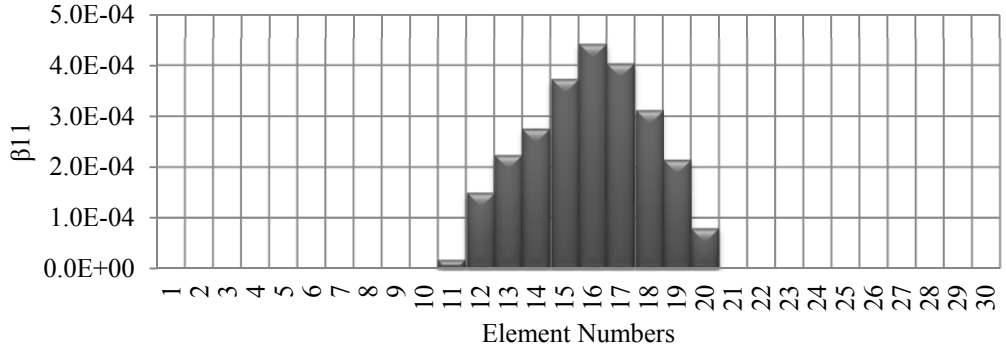

Figure 6: Damage localization results at ES_1 of case study 1 with respect to BL_P

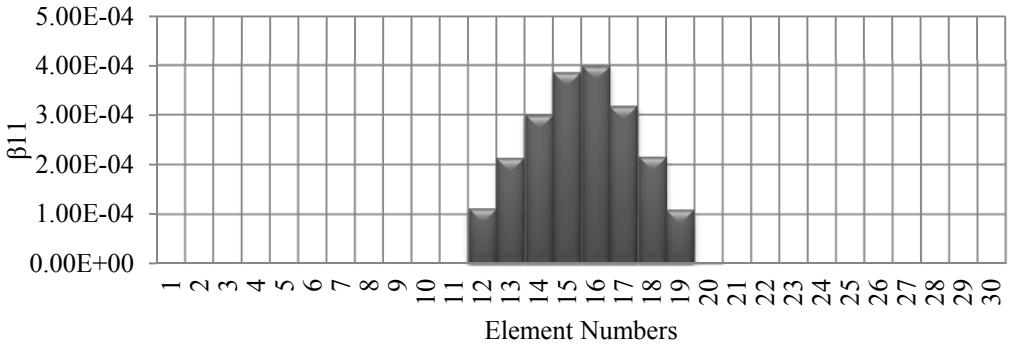

Figure 7: Damage localization results at ES_2 of case study 1 with respect to BL_P

3.2.2. Damage localization results using proposed baseline updating method

This section illustrates implementation of the proposed baseline updating method using the first case study as an example.

The damage assessment process of the baseline update method starts by defining the primary baseline similar to the constant baseline method. Frequencies and mode shapes of the first four modes of the undamaged RC beam are therefore used to define the primary baseline, BL_P, during the first step in phase 1 as given in Figure 1. Next, same vibration properties are measured at evaluations states to assess the structure using the MSEDI, β_j. Non-positive β_j values indicate that the structure has not been subjected to any sort of damage at the current

evaluation state from the time of defining the primary baseline. In such instances, phase 1 is repeated with the same primary baseline, BL_P. Indication of positive β_j values confirm that the structure has been damaged compared to the structural state at the time of defining the primary baseline.

Frequencies and mode shapes of the first four modes of the undamaged RC beam are used to define the primary baseline, BL_P as in step 1 in figure 1. Same vibration properties of the damaged RC beam after the first loading and unloading steps are used to define the first evaluation state, ES_1.

The damage index values, β_j, at ES_1, are then calculated to assess the structural condition during the third step. It should be noted that damage localization results at this instance are identical to Figure 6 and hence not repeated. Damaged elements at the end of first loading step are therefore identified as elements 11 to 20. The current evaluation state becomes the first damaged state, DS_1, as the RC beam is damaged.

Next, the matrix $[DE]_{30x1}$ is defined to save details of damaged elements at DS_1. Positive β_j values at elements 11-20 are saved into rows 11-20 of [DE] and all other entries are set to zero. The secondary baseline, BL_S, is then introduced as the last step of the phase 1 of the proposed damage assessment process. It should be noted that, BL_S equals to DS_1 for this case study.

The second phase of the proposed baseline updating method starts by defining two matrices $[DE^S]_{30x1}$ and $[DE^P]_{30x1}$. Both matrices are first set to $[DE]_{30x1}$. Then β_j values at each of the evaluation states are calculated with respect to the secondary baseline, BL_S, and the primary baseline, BL_P, until the next damaged state is detected. Positive β_j values with respect to BL_S are used to identify formation and/or propagation of cracks. Figure 8 indicates positive β_j values (with respect to BL_S) for elements 5-9 at ES_2 and hence detects the onset of the second

crack at quarter span. ES_2 therefore becomes the second damaged state, DS_2. Damage localization results using BL_P were previously presented in Figure 7. Comparison of Figure 7 and 8 clearly demonstrate that the proposed baseline updating method enables to successfully locate the newly damaged region in the RC beam and is hence superior to the existing constant baseline method.

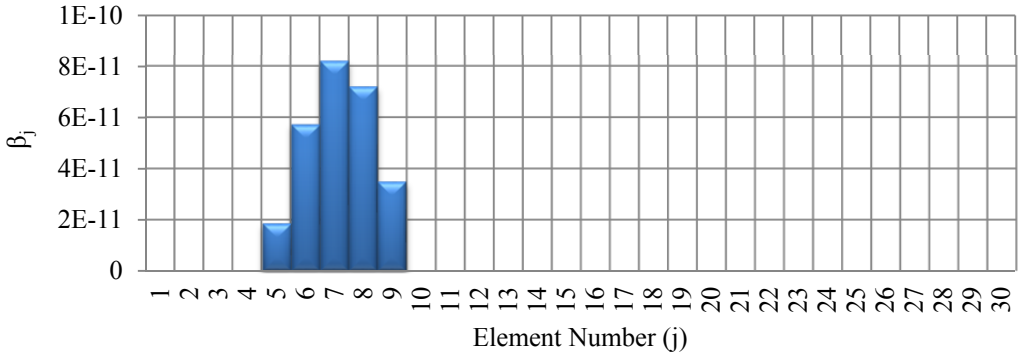

Figure 8: Damage localization results at ES_2 of case study 1 with respect to BL_S

Next, two new columns are added to matrices $[DE^P]$ and $[DE^S]$ to record positive damage index values of Figures 7 and 8, respectively, and to complete step 7. In step 8, the matrix [DE] is updated using Equation 5. The updated [DE] matrix can be used to identify all damaged elements that the structure has been subjected to during its service life. Figure 9 plots $\beta_{c,j}$ values of 30 row entries in [DE] column matrix against the element number after the onset of second crack at quarter span. Non-zero $\beta_{c,j}$ values imply that the j^{th} element has been subjected to damage compared to the initial state of the structure where the preliminary baseline was first established.

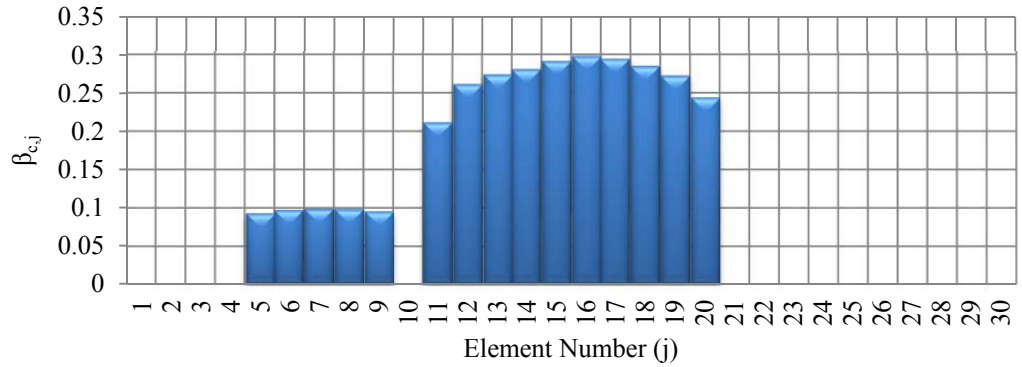

Figure 9: Identification of all damage elements using [DE] at ES_2

The next four case studies are used to confirm the improved damage localization ability of the proposed baseline updating method with different damage patterns.

3.3. Case study 2: Higher damage at quarter span followed by less damage at mid span

The second case study illustrates the damage localization ability of the proposed technique for detecting the onset of cracking at mid span in a cracked RC beam with damage at quarter span. The first crack is therefore simulated at quarter span and then the second crack with less severity (compared to the severity of first crack) was simulated at mid span.

W_1=60kN was applied at X_{W1} = 1.135m to create the first crack at quarter span. This state is denoted by ES_1 and later defined as DS_1 for the proposed baseline updating method. The ABAQUS smeared crack pattern and the damage localization results of β_j (using primary baseline, BL_P) are presented in Figure 10 and 11 respectively. β_j indicates positive values at elements 6-14, but does not indicate the sign of damage at elements 15-17. However, the overall damage localization result of β_j is acceptable as it has accurately localized the centre of the damaged zone around the quarter span.

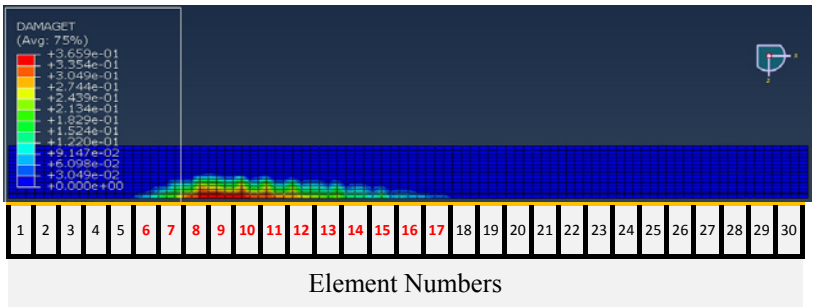

Figure 10: ES_1 of case study 2 - Cracked zone after first loading step

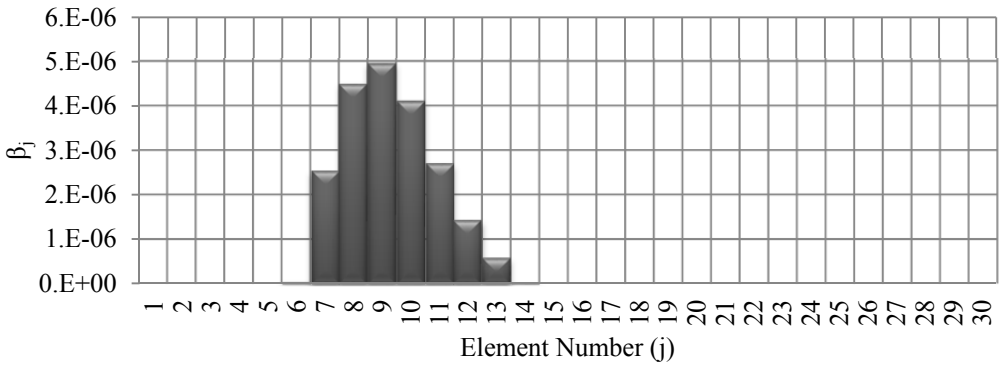

Figure 11: Damage localization results at ES_1 of case study 2 with respect to BL_P

W_2=36kN was then applied at X_{W2}=2.270m to create the second crack at the mid span with a smaller severity than the first crack. Figure 12 shows the smeared crack pattern obtained from the ABAQUS simulation. Figure 13 and 14 show the damage localization results using constant baseline and proposed baseline updating methods, respectively. Figure 15 plots $\beta_{c,j}$ values of the updated [DE] matrix after the onset of second crack at mid span and helps to identify all damaged elements.

Figure 13 has clearly identified the onset of second crack at mid span with clear peaks around elements 14-18. Figure 13 does not indicate any sign for presence of damage at mid span and hence indicates another failure of the constant baseline method for detecting the onset of the second crack.

This observation reassures that the proposed baseline updating method is superior to the constant baseline method. Further, it confirms that the improved damage localization ability of the proposed baseline updating method is independent of the sequence of damage occurrence and damage locations.

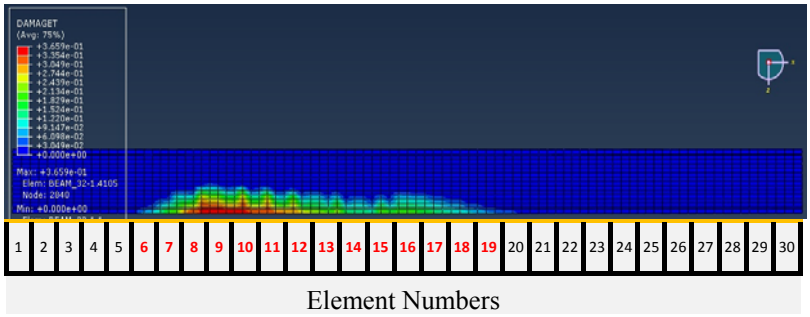

Figure 12: ES_2 of case study 2 - Cracked zone after second loading step

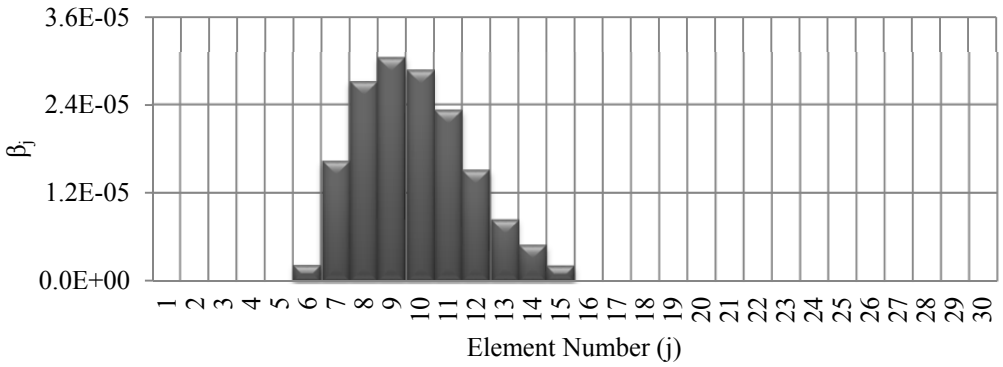

Figure 13: Damage localization results at ES_2 of case study 2 using BL_P

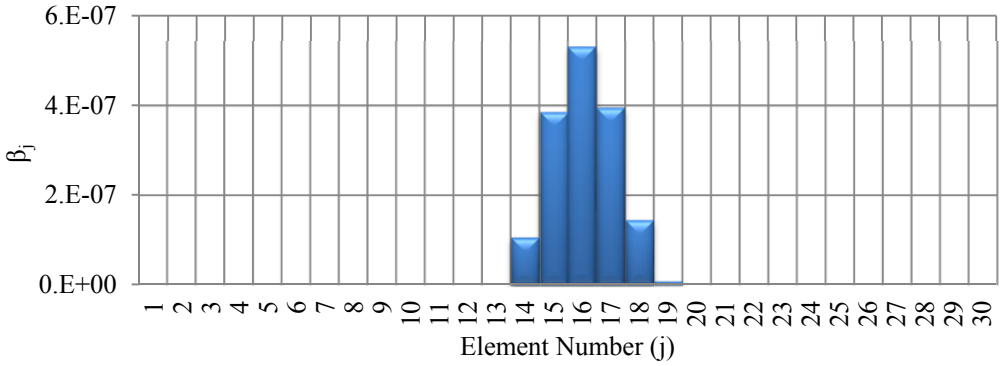

Figure 14: Damage localization results at ES_2 of case study 2 using BL_S

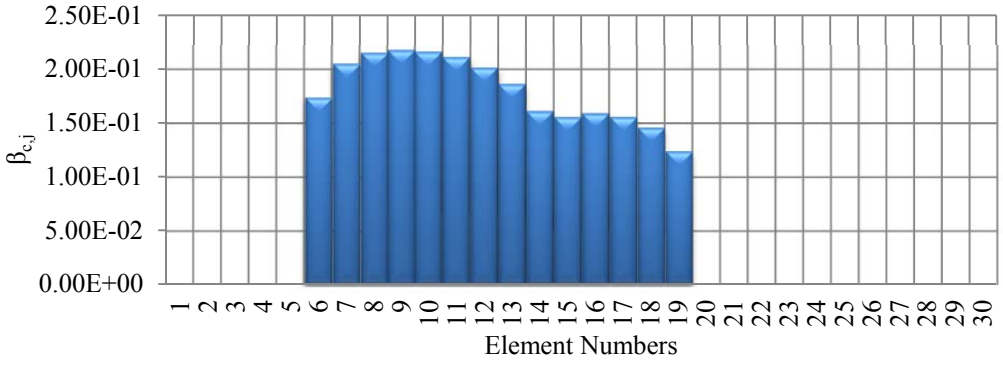

Figure 15: Identification of all damage elements using updated [DE] at ES_2 of case study 2

3.4. Case study 3: First crack at mid span; then at quarter span with similar severity

The third case study represents the formation of two low severity cracks at mid and quarter spans in that order of appearance. The first flexural crack was simulated at the mid span by applying W_1 = 30kN. Elements 13-19 were identified as damaged from the smeared crack pattern shown in Figure 16. This state is referred to as the first evaluation state, ES_1, and later called the first damaged state, DS_1, in the baseline updating method. β_j has successfully localized same elements with use of the undamaged state as the baseline, BL_P.

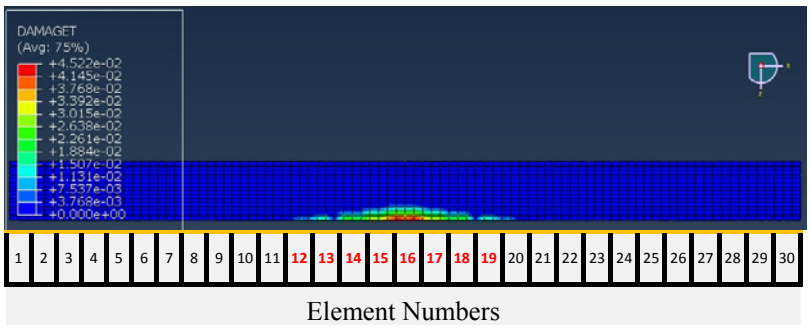

Figure 16: ES_1 of case study 3 - Cracked zone after first loading step

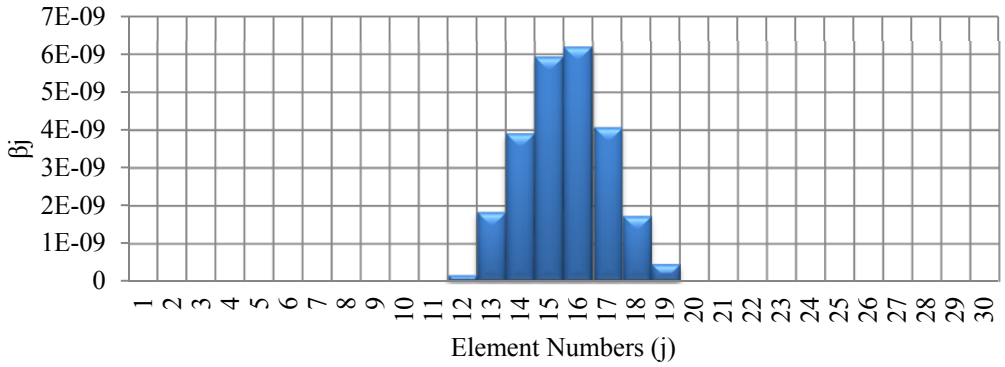

Figure 17: Damage localization results at ES_1 of case study 3 with respect to BL_P

W_2 = 42kN was then applied at X_{W2} = 1.135m to initiate the second crack at quarter span. Elements 7 - 11 are identified as forming the second cracking zone using the smeared cracking pattern shown in Figure 18. Figure 19 illustrates the damage localization results using the constant baseline method which has successfully localized both damage locations. However, the two previous case studies indicated that the constant baseline method does not localize the onset of the second crack, when the structure has already been subjected to a

larger damage. This implies that the constant baseline method can only detect the second crack once it propagates up to a similar damage severity as the first crack.

Figures 20 illustrates the damage localization results with updated baseline BL_S, which identifies the first damaged state DS_1. Second crack zone at quarter span is clearly localized indicating that the second crack has formed at quarter span. Figure 21 shows $\beta_{c,j}$ values of entries in the [DE] matrix at the evaluation state ES_2 and indicates both cracked zones.

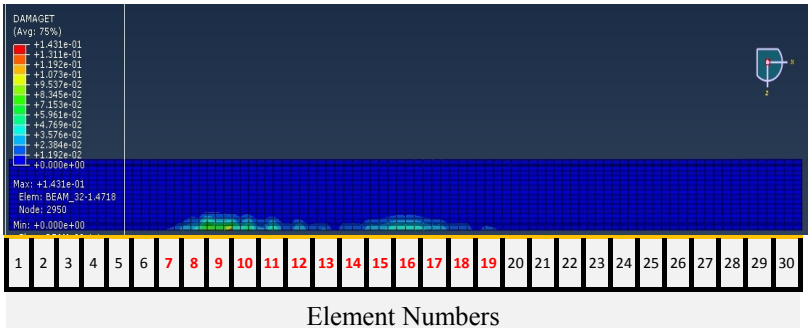

Figure 18: ES_2 of case study 3 - Cracked zone after second loading step

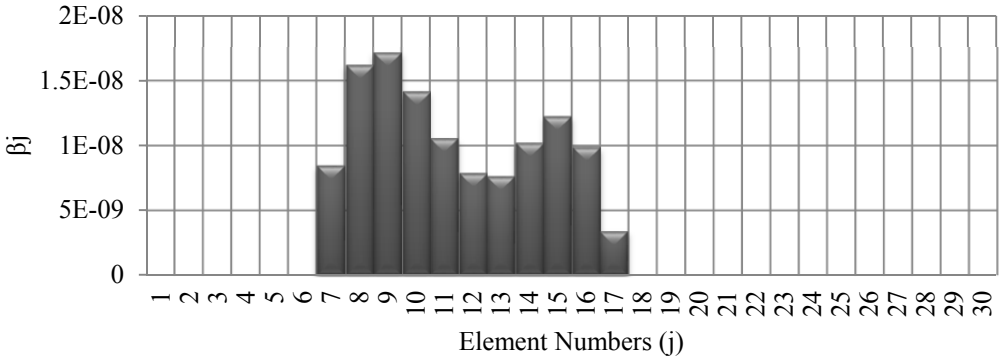

Figure 19: Damage localization results at ES_2 of case study 3 using BL_P

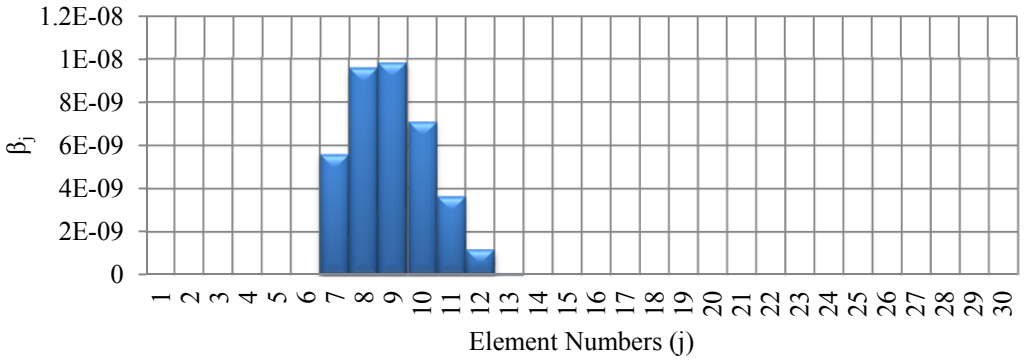

Figure 20: Damage localization results at ES_2 of case study 3 using BL_S

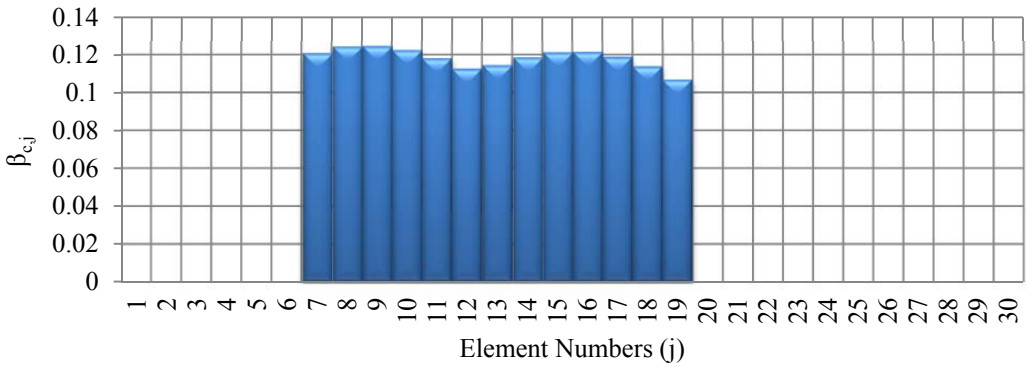

Figure 21: Identification of all damage elements using updated [DE] at ES_2 of case study 3

3.5. Case study 4: Smaller damage at quarter span followed by larger damage at mid span

The fourth case study was designed to create a smaller damage at quarter span followed by a larger damage at mid span. W_1, X_{W1}, W_2 and X_{W2} used in this case study were 30kN, 2.270m, 75kN and 1.135m, respectively. Figure 22 show the smeared crack pattern observed at the end of the first loading step, W_1. Figure 23 shows the corresponding damage localization result at this evaluation state (ES_1) using the preliminary baseline BL_P which agrees with the observed smeared crack pattern shown in Figure 22.

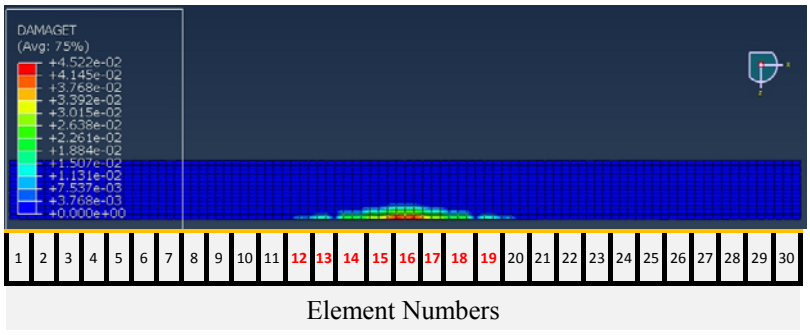

Figure 22: ES_1 of case study 4 - Cracked zone after first loading step

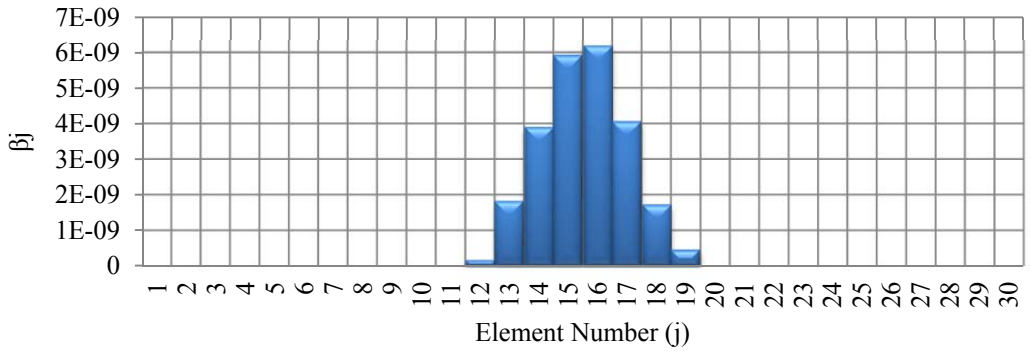

Figure 23: Damage localization results at ES_1 of case study 4 with respect to BL_P

Figure 24 is the observed smeared crack pattern after the second loading step. The constant baseline method has indicated positive β_j values at quarter span as shown in Figure 25. Figure 26 and 27 plot the entries in the second column in $[DE^S]$ matrix and entries in the updated [DE] matrix, respectively. Figure 26 detects the crack propagation at quarter span, whereas, Figure 27 shows both cracks at mid and quarter spans.

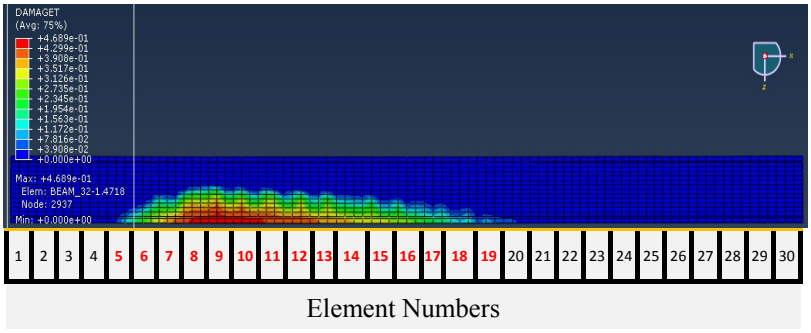

Figure 24: ES_2 of case study 4 - Cracked zone after second loading step

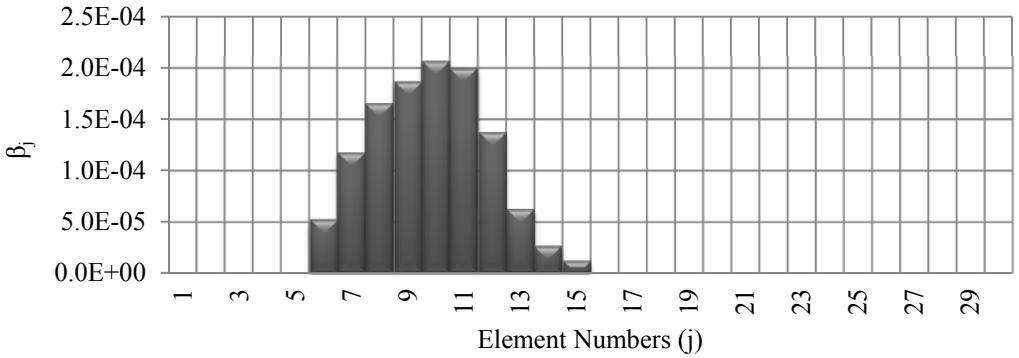

Figure 25: Damage localization results at ES_2 of case study 4 using BL_P

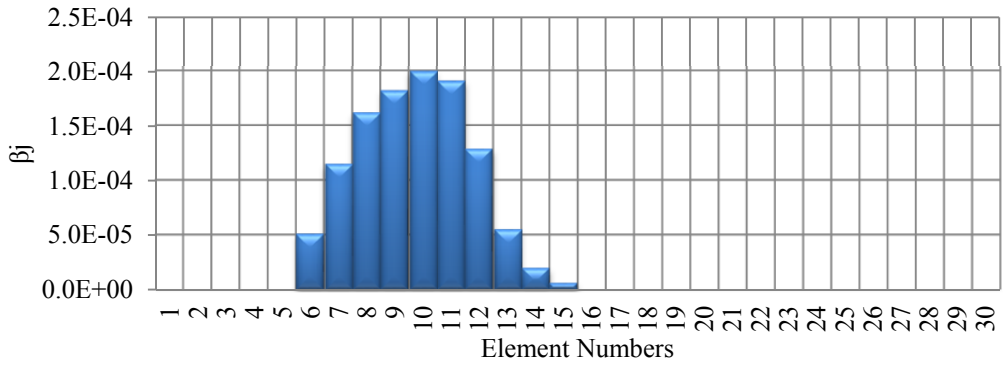

Figure 26: Damage localization results at ES_2 of case study 4 using BL_S

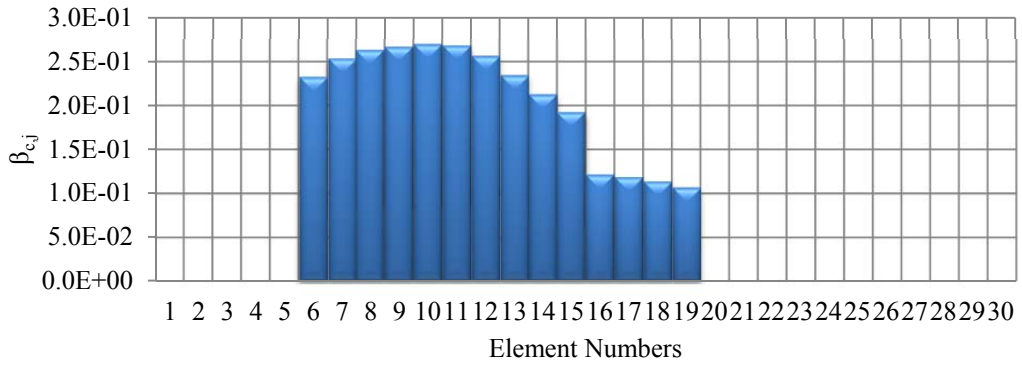

Figure 27: Identification of all damage elements using updated [DE] at ES_2 of case study 4

3.6. Case study 5: An example on continuous crack propagation and formation

The above four case studies illustrated that the proposed baseline updating method is superior to the existing constant baseline method in terms of locating crack formation. Further, they showed that the proposed baseline updating method has the ability to track the history of the crack formation. This case study (5) evaluates the ability of the proposed baseline updating method to locate both crack formation and propagation.

In this case study, cracks were simulated in a sequential order by varying the magnitude of loads, W_1, W_2 and W_3 at three locations, L/2, L/4 and 5L/6 (i.e. X_{W1} = L/2, X_{W2} = L/4 and X_{W3} = 5L/6) respectively to form new cracks and propagate existing cracks in six stages. The first crack was created at the mid span (at L/2 or X_{W1} = 2.270m) by applying a concentrated load, W_1 = 30kN. This was followed by applying the second load, W_2 = 42kN at X_{W2} =

1.135m to initiate the second crack at quarter span (i.e. L/4). The load, W_2 was then increased up to 54kN to propagate the second crack to a greater extent than the first crack. In the fourth stage, W_1 was increased up to 36kN and hence propagation of the mid span damage was simulated. In the fifth loading step, both W1 and W2 were increased to 42kN and 60kN so that both cracks at mid and quarter spans were propagated further. The sixth stage demonstrates initiation of a new crack at a 5L/6 (i.e. X_{W3} = 3.783m) due to a concentrated load W3=60kN. Figure 28 summarise the loading sequence followed in this case study.

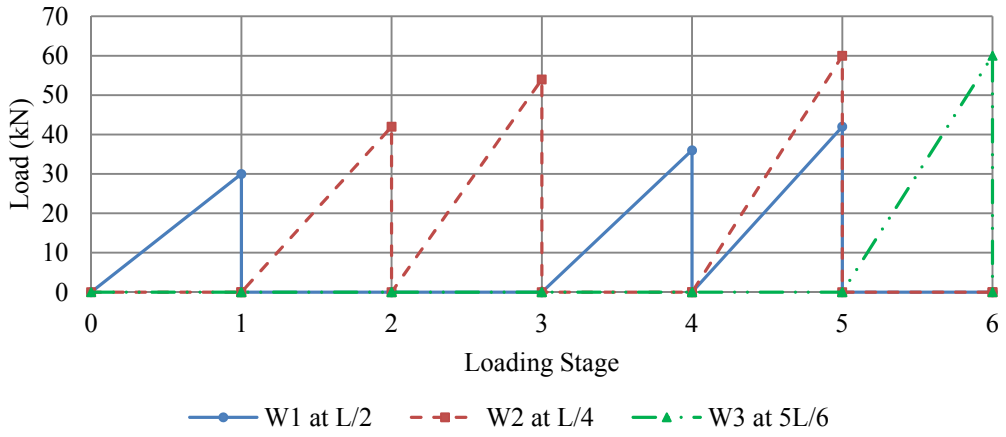

Figure 28: Loading Sequence

3.6.1. Localizing first two cracks

The damage localization results at the end of the first two loading stages were previously reported in section 3.4 and hence not repeated here.

3.6.2. Localizing propagation of the crack at quarter span

Figure 29 illustrates the smeared crack pattern observed at end of the third loading stage. Figure 18 is the smeared crack pattern observed at end of the second loading stage. Comparison of Figures 18 and 29 clearly indicates that crack at the quarter span has been propagated due to the increased magnitude of W_2.

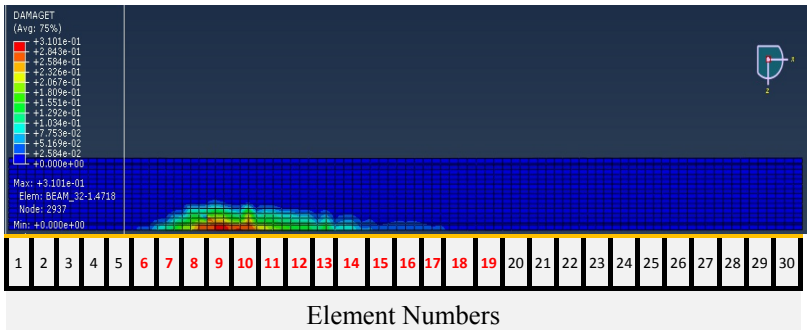

Figure 29: Smeared crack pattern at end of the third loading stage

Figure 30 illustrates the damage localization result of the proposed baseline updating method. It should be noted that this result is based on the updated secondary baseline at the end of the second loading stage (i.e. the damaged state shown in Figure 18). Figure 30 clearly indicates positive values around the quarter span of the beam and hence correctly localized the propagation of the existing crack. $\beta_{c,j}$ values of entries in the updated [DE] matrix at end of the third loading stage can be used to locate all damaged elements as shown in Figure 31.

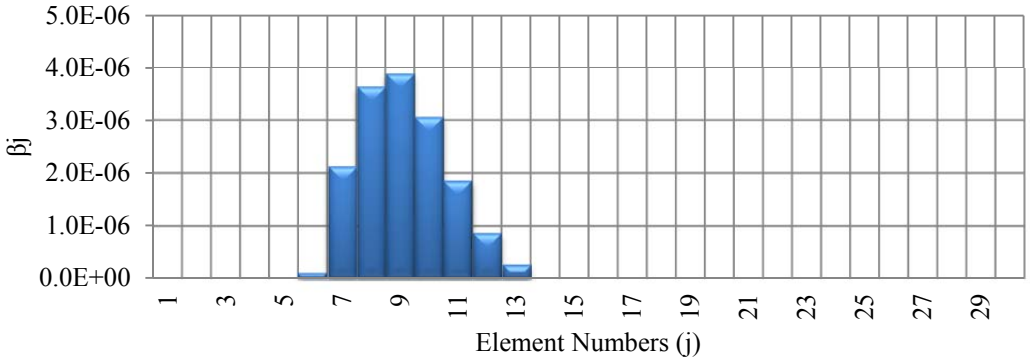

Figure 30: Localization of crack propagation at end of the third loading stage

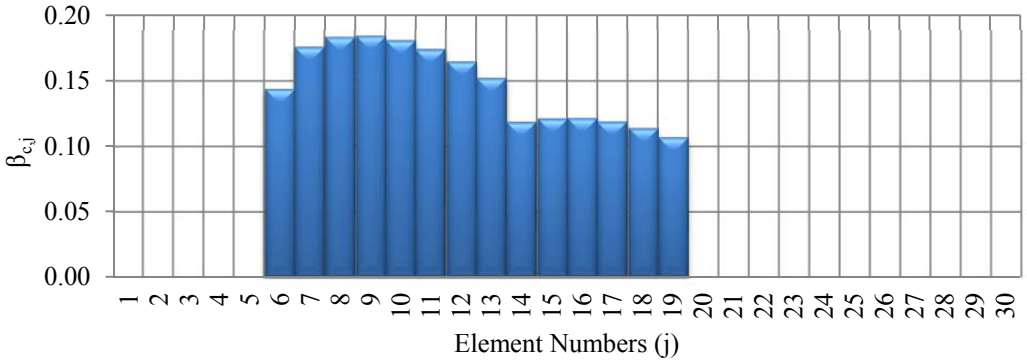

Figure 31: Identification of all damage elements using updated [DE]-Third loading stage of case study 5

3.6.3. Localizing propagation of the crack at mid span

Figure 32 indicates that the crack at mid span has been propagated from the previous state shown in Figure 30. The secondary baseline is updated for the previous damaged state shown in Figure 30 in the proposed baseline updating method. Figure 33 shows the damage localization results of the proposed baseline updating method at this loading stage and using the updated secondary baseline. It clearly detects the crack propagation at mid span. Figure 34 shows $\beta_{c,j}$ values of entries in the updated [DE] matrix at end of the fourth loading stage.

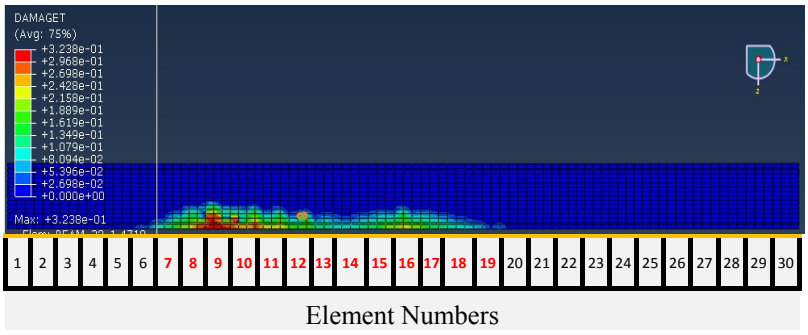

Figure 32: Smeared crack pattern at end of the third loading stage

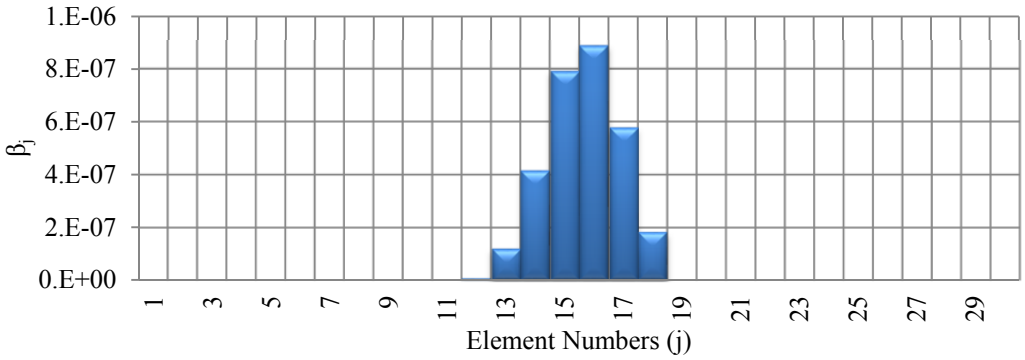

Figure 33: Localization of crack propagation at end of the fourth loading stage

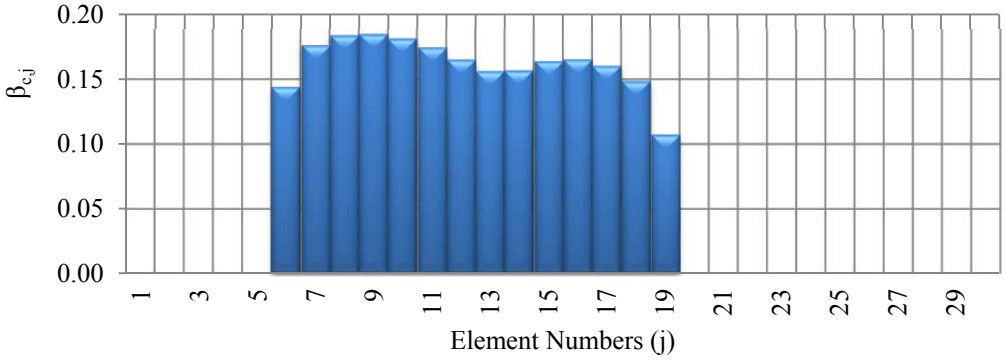

Figure 34: Identification of all damage elements using updated [DE]-Fourth loading stage of case study 5

3.6.4. Localizing propagation of the cracks at mid and quarter spans

Damage localization results obtained at the ends of the third and fourth loading stages therefore confirm that the proposed baseline updating method has the ability to locate the propagation of existing cracks irrespective of their locations. The fifth study represents a typical case where both cracks propagate simultaneously. Figure 35 is the smeared crack pattern obtained at the end of the fifth loading stage. Damage localization results shown in Figure 36 comply with the change in smeared crack pattern between Figures 35 and 32. This confirms that the proposed baseline updating method can successfully locate propagation of both cracks when they propagate simultaneously. Figure 37 shows the $\beta_{c,j}$ values of entries in the updated [DE] matrix at the end of the fifth loading stage.

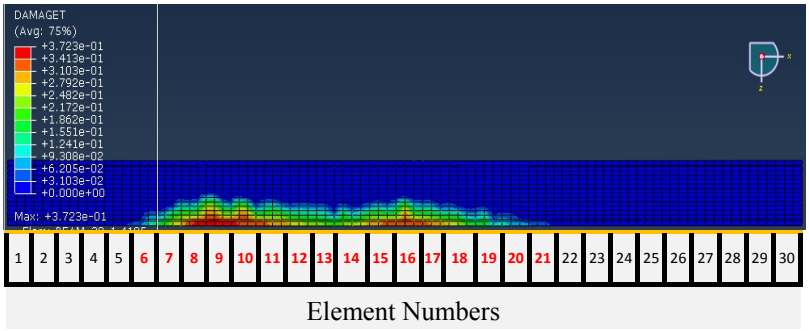

Figure 35: Smeared crack pattern at end of the fifth loading stage

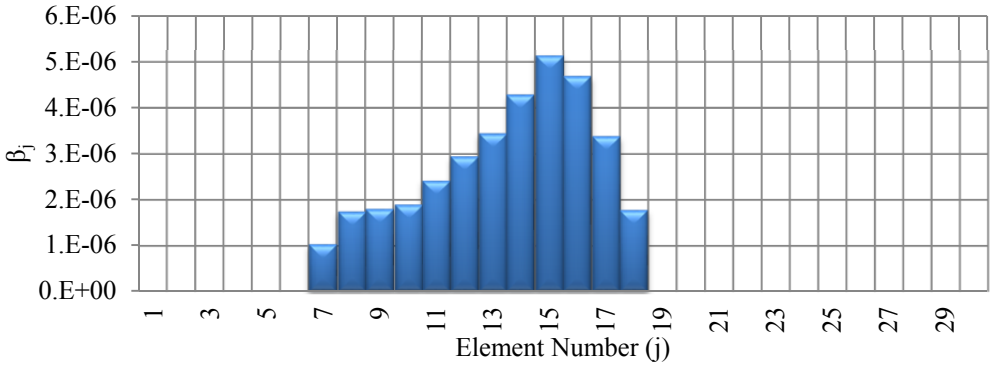

Figure 36: Localization of crack propagation at end of the fifth loading stage

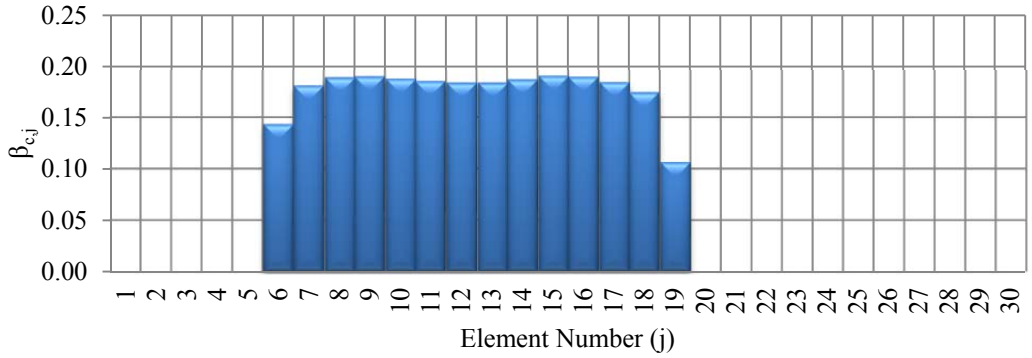

Figure 37: Identification of all damage elements using updated [DE]-Fifth loading stage of case study 5

3.6.5. Localizing formation of a new crack at a third point

The last loading stage was designed to create a new crack at 5L/6 of the damaged RC beam. The observed smeared crack pattern as shown in Figure 38 indicates the formation of a new crack around elements 23-26. Damage localization results of the proposed baseline updating method as shown in Figure 39, comply with this observation by indicating positive β_j values at elements 21-27. This demonstrates that the proposed baseline update method has the ability to detect formation of new cracks at any loading stage of the structure.

Figure 40 which plots $\beta_{c,j}$ values of entries in the [DE] matrix can be used to identify all of the damaged elements at end of the sixth loading stage. Figure 41 plots entries in the [DE] matrix, $DE_{j,1}$ values, which fail to visualise the damaged elements at the third point, even though positive values have been recorded between element 21 and 27. This indicates that use of $DE_{j,1}$ alone has lower visual diagnosis ability than the damage localization results obtained using $\beta_{c,j}$ values. The $\beta_{c,j}$ is therefore recommended to be used instead of using the entries in the [DE] matrix alone during localization of all damaged elements at the time of evaluation.

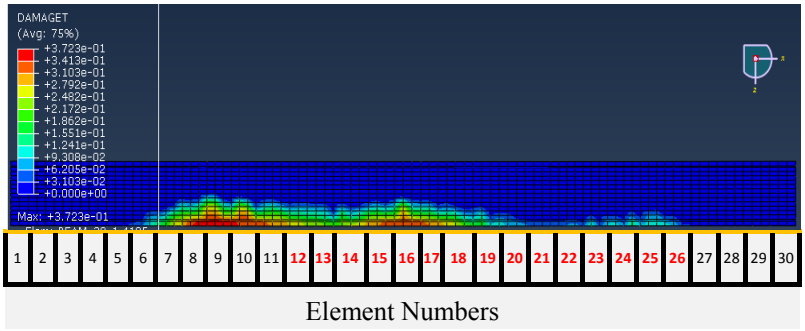

Figure 38: Smeared crack pattern at end of the sixth loading stage

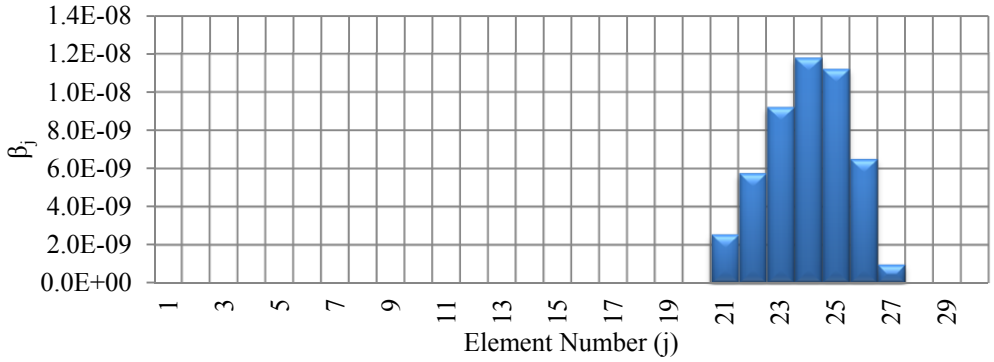

Figure 39: Localization the formation of the third crack at end of the sixth loading stage

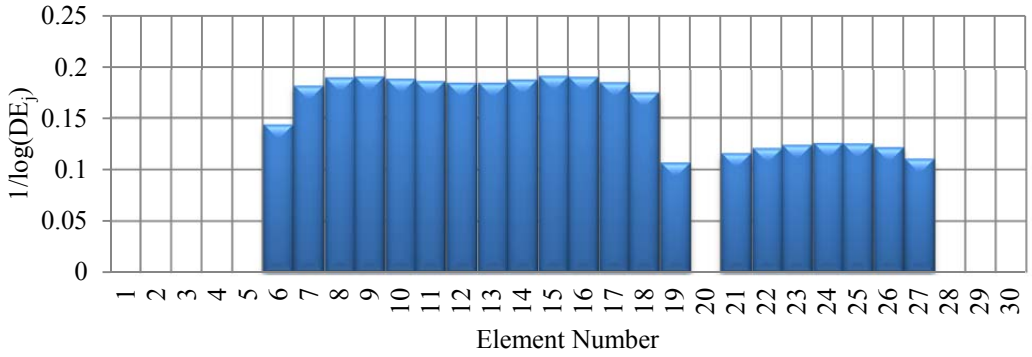

Figure 40: Identification of all damage elements using $\beta_{c,j}$-Sixth loading stage of case study 5

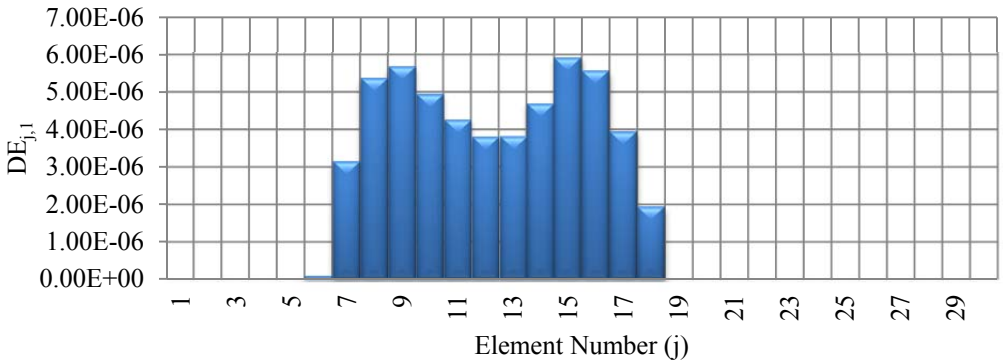

Figure 41: Identification of all damage elements using updated $[DE]_{j,I}$ entries -Sixth loading stage of case study

Conclusions

Although vibration based damage assessment techniques have been widely researched in recent years, their potential to assess damage in RC structures has not been fully explored. RC structures are predominantly subjected to flexural cracks which are non-uniformly distributed along orthogonal directions and hence add difficulties in the damage assessment process. The damage assessment process using the damage index method which is the simplest form of VBDAT, makes use of changes in vibration properties at evaluation state with respect to a previously known or baseline state. Existing damage index methods use a constant baseline, preferably that pertaining to vibration properties at the undamaged state, throughout the damage assessment process and hence they are referred to as the constant baseline methods. Results of this paper clearly indicate that the use of a constant baseline undermines the damage assessment ability of MSEDI with respect to flexural cracks in RC structures. The novel baseline updating method presented in this paper, on the other hand, has the potential to detect both crack formation and propagation and therefore is recommended for future applications.

Reference:

[1] C.R. Farrar, S.W. Doebling, An overview of modal-based damage identification methods, in: Proceedings of the DAMAS Conference, Sheffield, UK, 1997.

[2] M. Saleshi, R. Ziaei, M. Ghayour, M. Vaziry, A non model-based damage detection technique using dynamically measured flexiblity matrix, Iranian Journal of Science and Technology Transaction B-Engineering, 35 (2011) 1-13.

[3] Q. Huang, P. Gardoni, S. Hurlebaus, A probabilistic damage detection approach using vibration-based nondestructive testing, Structural Safety, 38 (2012) 11-21.

[4] T.M. Whalen, The behavior of higher order mode shape derivatives in damaged, beam-like structures, Journal of Sound and Vibration, 309 (2008) 426-464.

[5] M. Abdel Wahab, G. De Roeck, Damage detection in bridges using modal curvatures: application to a real damage scenario, Journal of Sound and Vibration, 226 (1999) 217-235.

[6] A. Alvandi, C. Cremona, Assessment of vibration-based damage identification techniques, Journal of Sound and Vibration, 292 (2006) 179-202.

[7] S. Chinchalkar, Determination of crack location in beams using natural frequencies, Journal of Sound and Vibration, 247 (2001) 417-429.

[8] B.L. Wahalathantri, Damage assessment in reinforced concrete flexural members using modal strain energy based method, in: PhD thesis, School of Civil Engineering and Built Environment, Queensland University of Technology, Brisbane, Australia, 2012.

[9] G. Owolabi, A. Swamidas, R. Seshadri, Crack detection in beams using changes in frequencies and amplitudes of frequency response functions, Journal of Sound and Vibration, 265 (2003) 1-22.

[10] D. Patil, S. Maiti, Experimental verification of a method of detection of multiple cracks in beams based on frequency measurements, Journal of Sound and Vibration, 281 (2005) 439-451.

[11] B. Nandwana, S. Maiti, Detection of the location and size of a crack in stepped cantilever beams based on measurements of natural frequencies, Journal of Sound and Vibration, 203 (1997) 435-446.

[12] H.A. Razak, F. Choi, The effect of corrosion on the natural frequency and modal damping of reinforced concrete beams, Engineering structures, 23 (2001) 1126-1133.

[13] R. Curadelli, J. Riera, D. Ambrosini, M. Amani, Damage detection by means of structural damping identification, Engineering structures, 30 (2008) 3497-3504.

[14] A.A. Elshafey, H. Marzouk, M. Haddara, Experimental damage identification using modified mode shape difference, Journal of Marine Science and Application, 10 (2011) 150-155.

[15] R.J. Allemang, The modal assurance criterion–twenty years of use and abuse, Sound and Vibration, 37 (2003) 14-23.

[16] M. Yuen, A numerical study of the eigenparameters of a damaged cantilever, Journal of Sound and Vibration, 103 (1985) 301-310.

[17] O. Salawu, Non-destructive assessment of structures using the integrity index method applied to a concrete highway bridge, Insight, 37 (1995) 875-878.

[18] A.K. Pandey, Biswas, M., and Samman M. M. , Damage detection in bridges from changes in curvature mode shapes, Journal of Sound and Vibration, 145 (1991) 312–332.

[19] A. Dutta, S. Talukdar, Damage detection in bridges using accurate modal parameters, Finite Elements in Analysis and Design, 40 (2004) 287-304.

[20] A. Pandey, M. Biswas, Damage detection in structures using changes in flexibility, Journal of Sound and Vibration, 169 (1994) 3-17.

[21] A. Patjawit, W. Kanok-Nukulchai, Health monitoring of highway bridges based on a Global Flexibility Index, Engineering structures, 27 (2005) 1385-1391.

[22] Z. Zhang, and Aktan, A. E., The damage indices for constructed facilities, in: Proceedings of the IMAC, 1995, pp. 1520–1529.

[23] N. Stubbs, J. Kim, K. Topole, An efficient and robust algorithm for damage localization in offshore platforms, in: Proceedings ASCE 10th Structures Congress, 1992, pp. 543-546.

[24] P. Cornwell, S. Doebling, C. Farrar, Application of the strain energy damage detection method to plate-like structures, Journal of Sound and Vibration, 224 (1999) 359-374.

[25] H.W. Shih, D.P. Thambiratnam, T.H.T. Chan, Vibration based structural damage detection in flexural members using multi-criteria approach, Journal of Sound and Vibration, 323 (2009) 645-661.

[26] B.L. Wahalathantri, D.P. Thambiratnam, T.H.T. Chan, S. Fawzia, An improved method to detect damage using modal strain energy based damage index, Advances in Strucural Engineering, 15 (2012) 727-742.

[27] L.S. Lee, V.M. Karbhari, C. Sikorsky, Investigation of integrity and effectiveness of RC bridge deck rehabilitation with CFRP composites, SSRP, (2004) 08.

[28] Abaqus v. 6.8 [Software], in, Dassault Systèmes Simulia Corp. [SIMULIA], , 2008.

[29] B.L. Wahalathantri, D.P. Thambiratnam, T.H.T. Chan, S. Fawzia, A material model for flexural crack simulation in reinforced concrete elements using ABAQUS, in: Proceedings of the eddBE2011 Conference, Queensland University of Technology, Brisbane, Australia, 2011, pp. 260-264.